

HYBRID TECHNIQUES FOR THE SEGMENTATION INFECTION WITH COVID-19 IN THE LUNGS USING CT IMAGES

Laxmibai Research Scholar, Sharnbasva University Kalaburagi.

Dr. Vinita Patil Prof , Dept. of Electronics & Communication Engineering, Sharnbasva University Kalaburagi. Email : laxmi.r1990@gmail.com ; vinita.pratapur@gmail.com

Abstract.

COVID-19 is a deadly disease which causes infection in both animals and human beings. It is a zoonotic disease that scatters worldwide in the beginning of the year 2020. COVID-19 is termed as Corona Virus Infection in 2019 that makes the whole world to suffer from this existential infection. The Chest x-rays detect lung pollution automatically. Images from computed tomography that aid in the struggle against COVID-19. Several demands are created during the separation of the diseased component from the X-ray slices, including a large difference in disease characteristic and a low intensity difference between infected and normal tissues. The deep model's pedagogy makes it hard to gather a large amount of a large amount of data in a short period of time. For Addressing the separation of COVID-19 related lung disease by using Seg-Net It is proposed that the damaged areas of the chest X-ray be automatically analysed scan, using image process technique to automate the operation to increase the efficiency of the system.

Keywords. Datacenter architecture, datacenter energy efficiency, energy efficient measures, and calculation of datacenter carbon footprint.

1. INTRODUCTION

Medical imaging, such as X-ray or computed tomography, can be used as an alternative to the established polymerase chain reaction of reverse transcription (RT-PCR) as a conventional strategy for COVID-19 screening or monitoring (CT). Medical imaging technology has advanced significantly in the last several years now a widely utilized approach for diagnosis as well as quantified evaluation of a variety of disorders Chest CT scanning, in particular, has established as a common diagnostic technique for pneumonia. As a result, chest CT imaging is strongly advised for COVID-19 diagnosis and follow-up. Furthermore, CT imaging is being used to investigate COVID-19 quantitation as well as disease monitoring [1].

On the contrary, chest Computed tomography (CT) or X-ray (CT) imaging are thought to be quicker and more complementing methods for early detection of COVID-19 infections. CT imaging, on the other hand, outperforms X-ray radiography in terms of revealing greater structural/anatomical features of the lung [2]. Chest CT scans exhibit a sensitivity of 0.97 in the diagnosis of COVID-19, allowing for the detection of radiological patterns such as ground-glass on all sides and on the periphery opacities and patchy consolidations in infected patients' lungs. Furthermore, quantitative analysis of CT scans gives crucial information regarding the extent of lesions and the severity of the illness, with effective lung CT image segmentation serving as a necessary preparatory step [3].

The initial laboratory testing approach for COVID-19 diagnosis is RT-PCR stands for reverse polymerase chain reaction (transcription polymerase chain reaction). Coronavirus

is made up entirely of RNA (ribonucleic acid), which must For amplification, it must be transformed to DNA (deoxyribonucleic acid) and virus detection through RT-PCR. Apart from its benefits, it is time-consuming, this might result in the disease spreading further from the sick individual, and the deep nasal swabs are inconvenient. Early detection of the illness is critical for isolating positive individuals and avoiding community spread [4].

2. GENERATE A CONTRAST METRIC

Original CT-scan pictures show bright areas in an image to add substantial visible information. However, certain areas are very bright, while others are overly dark. In order to return a more accurate segmentation, it is required to boost local contrast prior to categorizing details. COVID-19 targets, in general, exhibit positive local contrast, which indicates that the lesion regions are brighter than the nearby backdrop in all directions. We offer two enhancement functions to regulate the appropriate brightness level. Exponential function, and ii) a logarithmic function the exponential function raises local contrast somewhat and may if the exponential parameter is if the exponential parameter is set, the function may be utilised as a preventative measure to (1.0). A logarithmic term is used in another suggested function. It in dark areas, enhances local contrast while preserving local contrast in a bright environment regions. By merging two upgraded characteristics, the key facts may be viewed and written as:

$$Y_{i,j} = (L - 1) \cdot \left(\frac{E_{i,j} - \min\{E_{i,j}\}}{\max\{E_{i,j} - \min\{E_{i,j}\}\}} \right) \quad (1)$$

$$E_{i,j} = \alpha A_{i,j} \cdot \beta B_{i,j} \quad (2)$$

$$A_{i,j} = \left(\frac{S_{i,j}^2}{|G_{i,j}| + \psi} \right)^{\gamma a} ; B_{i,j} = \log^{\gamma b} \left(1 + \frac{S_{i,j}^2}{|G_{i,j}| + \psi} \right) \quad (3)$$

$$|G_{i,j}| = \max_z |I_{i,j} \otimes f_{x,y,z}| \quad (4)$$

where $Y_{i,j}$ is a contrast metric that can be seen. The entire amount of luminance levels in a visible domain is denoted by L . $E_{i,j}$ is a metric for contrast. $A_{i,j}$ is a measure for linear contrast. $B_{i,j}$ is a contrast metric with a logarithmic scale. a metric of linear contrast constant a comparison of logarithmic contrast metrics $S_{i,j} - a$ structural picture that has been filtered (dilated) [15]. The linear contrast metric's contrast enhancement parameter. $\gamma b - a$ logarithmic contrast metric contrast enhancement parameter. f a tiny integer to avoid a computation mistake if any of the components of a directional gradient edge metric are equal to zero $|G_{i,j}|$ is a gradient edge metric with a directed gradient. $I_{i,j}$ is a source image. $f_{x,y,z}$ a direction directional compass mask (compass masks called the masks, which are formed by taking a single mask and spinning it to the eight basic compass directions). \otimes - a convolution operator in two dimensions.

When a structural element is supported by a height, general mathematics notions with dilation are [16]. As a result, the dilation of $A(x, y)$ by $B(x, y)$ is defined as follows:

$$(A \oplus B)(x, y) = \max_{(x', y') \in D_b} (A(x - x', y - y') + B(x - x', y - y')) \quad (5)$$

where A represents the original picture, B represents dilated features, and D represents a structural element (b). The Figure 1 shows a suggested masking pneumonia areas comparison using various structural filters.

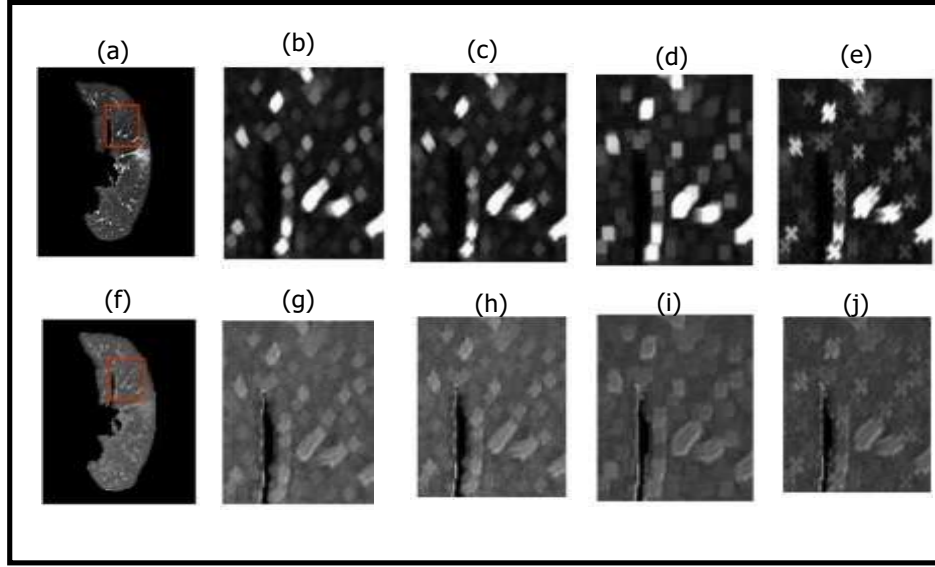


Fig. 1. The proposed masking pneumonia regions comparison; (a) a CT-scan image; (b) a dilated structural image by using a „circle“ dilating filter; (c) a dilated structural image by using a „plus“ dilating filter; (d) a dilated structural image by using a „square“ dilating filter; (e) a dilated structural image by using a „circle“ dilating filter; (f) a visualized contrast metric; (g) a visualized contrast metric by using a „circle“ dilating filter; (h) a visualized contrast metric by using a „plus“ dilating filter; (i) a visualized contrast metric by using a „square“ dilating filter; (j) a visualized contrast metric by using a „circle“ dilating filter.

3. TWO-DIMENSIONAL DECOMPOSITION IN EMPIRICALMODE (2DEMD)

2D EMD is a two-dimensional expansion of single-dimensional EMD. EMD breaks down a signal into its constituent parts distinct modes Intrinsic Mode Functions are what they're called (IMFs) [17,18]. Each IMF has the same length and the same amount extrema points and zero-crossing. The deconstructed signal envelopes act as oscillatory modes. The IMFs are non-orthogonal, yet they can sufficiently characterize the signal. Single-dimensional EMD is useful for natural signals (such as electrocardiogram data) because it can monitor their non-linearity and non-stationarity. The EMD signal provides the inherent characteristics of a signal.

In this section, we will first look at the study of single dimensional EMD. The signal values for a one-dimensional EMD are set with regard to time (t). The time (t) parameter is used to describe how long it takes for something to happen is used to describe how long it takes for something to happen will be converted based on the sample size in the signal is represented digitally (n). However, for the sake of simplicity, we will examine a time (t) variable signal. The signal's minimum and maximum points $f(t)$ can be linked to get the curvature of the lower envelope ($f_l(t)$) and the upper envelope curve ($f_u(t)$). $Y = (f_u(t) + f_l(t))/2$ is the average of the results two signals. The first proto-IMF signal, $W_1(t)$, is obtained by subtracting the arithmetic mean of the original signal ($f(t)$):

$$W_1(t) = f(t) - Y(t) \quad (6)$$

$W_1(t)$, the proto-IMF signal, then passes through a filtering process up to a threshold point. The conditions for a Function of Intrinsic Mode (IMF) are met at this stage. These stages result in the very first IMF signal (s_1). Following the first step, the relevant residue signal, ($r_1(t)$), is,

$$r_1(t) = f(t) - S_1(t) \quad (7)$$

Similarly, applying the filtering procedure on the first residue signal ($r_1(t)$) yields second, third, and so on IMFs. Generally,

$$r_{j-1}(t) - S_j(t) = r_j(t); j = 1, 2, 3, 4, \dots, N \quad (8)$$

N specifies the number of IMFs in this case. Finally, a residue signal ($r_N(t)$) and a collection of IMFs ($s_1(t), s_2(t), \dots, s_N(t)$) are produced, resulting in

$$f(t) = \sum_{j=1}^N S_j(t) + r_N(t) \quad (9)$$

In this case, $S_j(t)$ is the j^{th} order IMF. Lower-order IMFs are similar to high-frequency modes, whereas higher-order IMFs are similar to low-frequency modes [17].

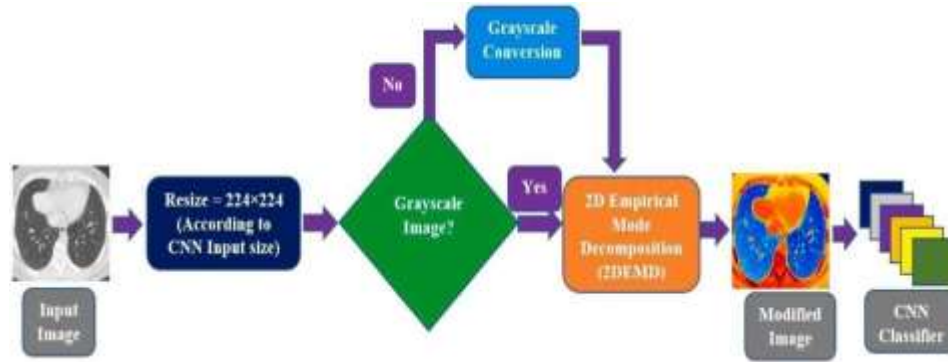


Fig. 2. The proposed method for SARS-CoV-2 patient classification. The original CT scan/Chest X-ray picture is first scaled according to the CNN classifier's input criteria. The picture is then transformed to a gray-scale image (if it is not already). The 2DEMD method then decomposes the picture into individual IMFs, which are then easily added together to create a modified version of the original medical image. After that, the CNN is used to learn and classify features from the updated picture.

This section provides an overview of the suggested technique as well as a full description of feature extraction methods and CNN training. The suggested technique is illustrated briefly in Fig. 2. To begin, any image is transformed to grayscale. Using two-dimensional Empirical Mode Decomposition, the CT-scan/Chest-X-ray picture is then decomposed into discrete Intrinsic Mode Functions at High and Low Frequencies (IMFs) (2DEMD). The purpose of employing the goal of 2DEMD is to capture tiny and high textural frequency profiles of CT-scan/Chest-X-ray pictures of the lung, which have SARS-CoV-2 patient-specific features.

4. FUZZY C-MEAN AUTOMATED REGION-GROWING SEGMENTATION (FARGS)

There are numerous ways to picture segmentation, the majority of which are dependent on expert opinion, which is a time-consuming procedure [19], whereas automated fuzzy c-mean area expanding segmentation is free of human-based knowledge. The grey level lungs CT-scan is separated into four equal portions during the preprocessing step, and a set of nearby pixels is used in the extraction of a recognized region of interest. The Histogram Stretch a filter is a device that is used to improve contrast (the grey level picture is turned into natural binary image format for

greater visibility). Finally, we employ a fuzzy c-mean segmentation method [20], which is primarily employed for pattern categorization. This segmentation method separates data into two halves. It is based on the objective function (OF) described below:

$$\tilde{y} = \sum_{i=1}^1 \sum_{j=1}^c \frac{5_{ij}}{\sum_{j=1}^c 5_{ij}} \|y_i - C_j\|^2 \quad (10)$$

where $1 \leq q \leq \infty$ and a real integer, 5_{ij} is the degree to which a person is a member of y_i in cluster C_j , y_i is the i th dimensional data that has been measured, j is the cluster's dimensional centre, and is any average representing the likeness between any measured data and the centre. Fuzzy partitioning is accomplished by frequent updates of the OF, as well as the renewal of membership 5_{ij} and cluster centers C_j by:

$$5_{ij} = \frac{1}{\sum_{j=1}^c \left(\frac{\|y_i - C_j\|}{\|y_i - C_k\|} \right)^{\frac{2}{g-1}}} \quad (11)$$

$$C_j = \frac{\sum_{i=1}^1 \frac{5_{ij}}{\sum_{j=1}^c 5_{ij}} y_i}{\sum_{i=1}^1 \frac{5_{ij}}{\sum_{j=1}^c 5_{ij}}} \quad (12)$$

The repeat stops if the following condition holds: $\{ |5^{(k+1)}_{ij} - 5^{(k)}_{ij}| \} < \div$, where \div is an

elimination criterion ranging from 0 to 1, and k is the number of repetition steps. This strategy yields a local minimum of \tilde{y}_q . Finally, as seen in Fig.3 below, the FARGS technique is applied to the lungs disorder dataset.

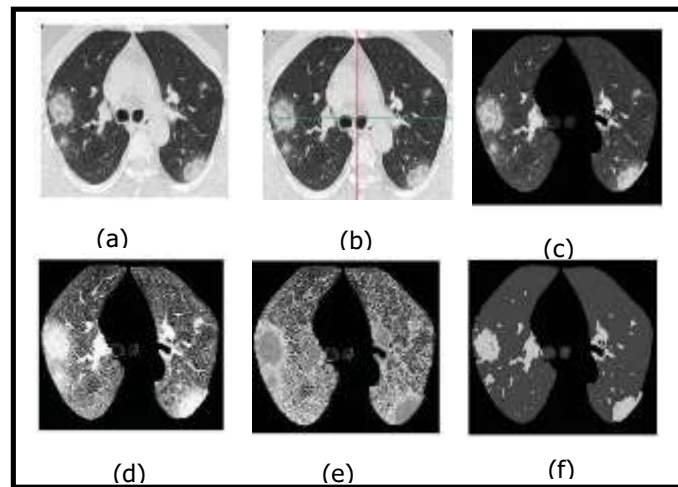


Figure 3: Automated region-growing segmentation with a fuzzy c-mean (FARGS) framework for COVID-19. (a) Lung's image (gray level), (b) Lung's image (segmented), (c) Lung's image (ROI extraction), (d) Lung's image (histogram stretch), (e) Lung's image (gray to natural binary), (f) Lung's image (fuzzy c-mean segmentation)

5. STRUCTURE AND TEXTURE COMPONENT EXTRACTION

Each image can contain information such as the form of the item (or the homogeneous section) in the image as well as a texture, which can also contain information useful in some computer vision applications. The texture component is utilized as input to the proposed encoder–decoder neural networks in this case. To do this, preprocessing is used to remove the texture component. The interval gradient is used for gradient smoothing that is adaptive in the structure–texture decomposition approach presented in [21]. It is a technique that divides an image f into $S + T$ ($f = S + T$) of a limited variation component (Structure) and a component that contains the picture's oscillation part (Texture/Noise) [22]. On the CT-scan pictures, we used this procedure. The texture and structural components are then used as inputs to the suggested encoder–decoder model. The structural component is extracted using gradient rescaling using interval gradients, followed by a color management technique.

The gradients inside texture areas should be suppressed to obtain a texture-free signal from an input signal. Furthermore, for all local windows Ω_r , the signal should be rising or decreasing. We use the following formula to rescale the gradients of the input signal with the matching interval gradients to achieve these goals:

$$(A'I)_p = \begin{cases} (AI)_p \cdot w_p & \text{if } \text{sign}((AI)_p) = \text{sign}((A_n I)_p) \\ 0 & \text{otherwise} \end{cases} \quad (13)$$

where $(A'I)_p$ represents the rescaled gradient, and w_p is the rescaling weight

$$w_p = \frac{\min(1, |(AI)_p| + s_s)}{|(AI)_p| + s_s} \quad (14)$$

where s_s is a tiny constant used to avoid numerical instability. Too low s_s values would render the algorithm vulnerable to noise, contributing undesired artefacts to the filtering output. Increase s to lessen noise sensitivity, however textures may not be totally filtered if s_s is too large. In our implementation, we used $s_s = 10^{-4}$.

In the rescaling of gradients, stage (Eqs. (1) and (2)), we employ the gradient sums of color channels for filtering color pictures, that is:

$$w^p = \frac{\min(1, \sum_{c \in \{r, g, b\}} |(A \Omega^c I)_p| + s_s)}{\sum_{c \in \{r, g, b\}} |(A \Omega^c I)_p| + s_s} \quad (15)$$

Figure 4 displays filtering examples to illustrate how structure and texture extraction may be done using the same settings $c \in \{0.0001, 0.0009\}$.

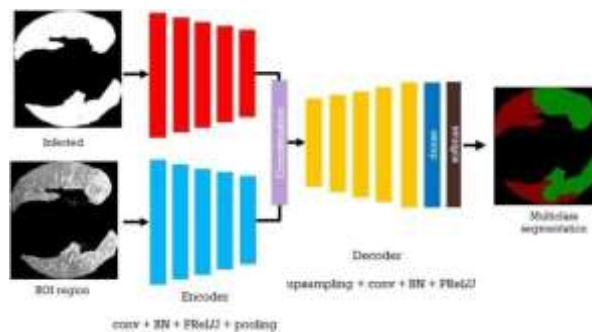


Fig. 4 Multi-class segmentation of the lung infected regions

The deep learning model's two-stream inputs are reflected by the findings of the first lung infection segmentation and the results of the second segmentation, this is the topic of discussion. This approach enables learning on a specific location as well as being more precise due to data limitations. Figure 4 depicts the deep learning model's input and output for multiclass segmentation at this level.

6. DEEP NEURAL NETWORKS

The general approach to semantically segmenting pictures is to develop a structure that collects features through consecutive convolutions and uses that knowledge to generate a segmentation map as an output. Figure 5 shows.

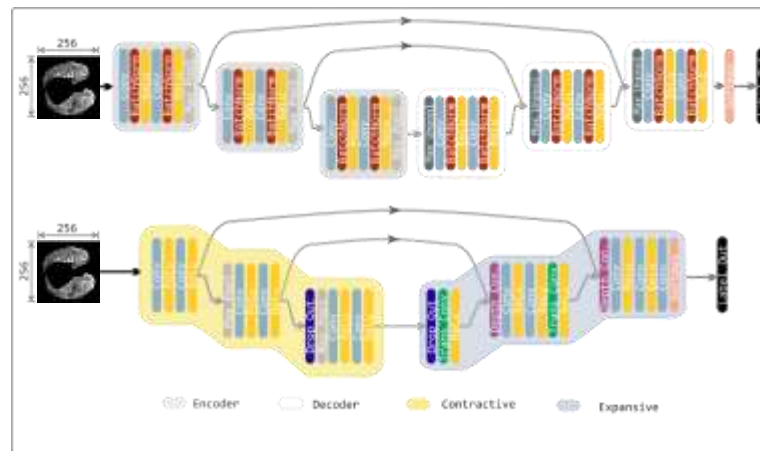


Fig. 3 The DNN architectures The SegNet (top) where the encoder-decoder of the network are illustrated using the gray and white bubbles, and U-NET (bottom) where the contractive and expansive layer patches are encapsulated in blue and yellow bubbles

6.1. U NET architecture

U-NET was first designed for medical picture comprehension and segmentation. It may be used in a variety of ways in the sector and is an important architecture in the medical imaging automation society. In this part, we go through the network's core technological aspects and how they contribute to successful outcomes. This network's design is divided into two parts: contractive and expansive. The contracting route is made up of many patches of convolutions with 3×3 filters and unity strides in both directions, followed by ReLU layers. This route extracts the important characteristics of the input and returns a feature vector of a predetermined length. The second route extracts information from the contractive path by copying and cropping, as well as from the feature vector using up-convolutions, and forms an output segmentation map via a subsequent operation. The operation that connects the first and second pathways is a critical component of this system. This connection enables the network to obtain very precise information from the contractive route, resulting in a segmentation mask that is as near to the intended output as feasible. [23] provides a full analysis of the architecture.

6.2. SegNet architecture

A Deep Neural Network (DNN) is a kind of neural network that uses deep learning to solve problems is used that was created to simulate scene segments such as the road picture segmentation tool. Because vast sections of road photos consist of classes like as road, sidewalk, and sky, the network must converge using highly unbalanced datasets. We proved statistically in

the dataset section how the dataset utilized in this work exhibits discrepancy in class representation. As a result, SegNet was our first option for this project. SegNet is a DNN with a lot of features a depth of three encoder-decoders. The encoder layers are the same as the VGG16 network's convolutional layers. The segmentation mask is constructed by the decoder using pooling indices from the corresponding encoder's max-pooling. To minimize complexity, the developers deleted the completely linked layers, reducing the number of parameters in the encoder sector from $1.34e+8$ to $1.47e+7$. See also [24].

7. COMPARATIVE ANALYSIS

Method	Description
Generate a contrast metric	Original CT-scan pictures show bright areas in an image to add substantial visible information. However, certain areas are very bright, while others are overly dark. In order to return a more accurate segmentation, it is necessary to boost local contrast prior to categorizing details.
Two-Dimensional Empirical Mode Decomposition(2DEMD)	2D EMD is a two-dimensional expansion of single-dimensional EMD. EMD decomposes a signal into distinct modes known as Intrinsic Mode Functions (IMFs). Each IMF has the same length and the same amount of zero-crossing and extreme points. The deconstructed signal envelopes act as oscillatory modes.
Fuzzy c-mean Automated Region-growing Segmentation (FARGS)	Fuzzy c-mean automated region expanding segmentation is free of human-based knowledge. The grey level lungs CT-scan is separated into four equal portions during the pre-processing step, and a set of nearby pixels is used to extract a recognized region of interest. The Histogram Stretch filter is used to improve contrast (the grey level picture is turned into natural binary image format for greater visibility).
Structure and Texture Component Extraction	Each image can contain information such as the form of the item (or the homogeneous section) in the image as well as a texture, which can also contain information useful in some computer vision applications. The texture component is utilized as input to the proposed encoder-decoder neural networks in this case. To do this, preprocessing is used to remove the texture component.
Deep neural networks U-NET architecture SegNet architecture	UNET was first designed for medical picture comprehension and segmentation. It has a wide range of applications in the sector and is an important architecture in the medical imaging automation society. In this part, we go through the network's core technological aspects and how they contribute to successful outcomes.
	gNet is a Deep Neural Network that was created to simulate scene segmentssuch as the road picture segmentation tool. Because vast sections of road photos consist of classes like as road, sidewalk, and sky, the network must convergeusing highly unbalanced datasets.

8. CONCLUSION

COVID-19 is a fatal illness that may infect both animals and humans. It is a zoonotic illness that

will spread around the planet at the start of the year 2020. COVID-19 is an acronym for Corona Virus Disease 2019, which causes this existential illness to afflict the whole globe. Chest computed tomography images identify lung pollution automatically, assisting in the treatment of COVID-19. Several demands are formed during the separation of the sick component from the X-ray slices, including a considerable difference in disease characteristics and a low intensity differential between infected tissue and normal tissues. Most automatic detection algorithms in recent improvements of SARS-CoV-2 detection and classification operate with the raw image of the CT-scan/Chest-X-ray picture. However, in this paper, a hybrid technique combining classical signal processing with deep learning methodology is used. The picture is transformed to a single channel (gray- scale) image, and then 2DEMD is applied to it. The leftover component of the decomposition is then removed, and all of the Intrinsic Mode Functions (IMFs) are combined to generate a modified CT-scan/Chest-X-ray picture.

9. REFERENCES

- [1] Rubin GD, Ryerson CJ, Haramati LB, Sverzellati N, Kanne JP, Raoof S, et al. The role of chest imaging in patient management during the COVID-19 pandemic. *Radiology* 2020;158:106–16. <https://doi.org/10.1148/radiol.2020201365>.
- [2] Fan D-P, Zhou T, Ji G-P, Zhou Y, Chen G, Fu H, et al. Inf-Net: Automatic COVID-19 Lung Infection Segmentation from CT Images. *IEEE Transactions on Medical Imaging*. 2020.
- [3] Wu Q, Wang S, Li L, Wu Q, Qian W, Hu Y, et al. Radiomics Analysis of Computed Tomography helps predict poor prognostic outcome in COVID-19. *Theranostics*. 2020;10:7231.
- [4] Siddiqui, Ahsan Ali. "The Need of Early Detection of Positive COVID-19 Patients in the Community by Viral Tests (eg RT-PCR Tests) and Antibody Tests (Serological Tests) to Stop the Spread." (2020).
- [5] Adel Oulefki, SosAgaian, ThaweesakTrongtirakul, AzzeddineKassahLaouar, Automatic COVID-19 lung infected region segmentation and measurement using CT-scans images, *Pattern Recognition, Volume 114*, 2021, 107747, ISSN0031-3203,
- [6] RaminRanjbarzadeh, SaeidJafarzadehGhouschi, Malika Bendeache, Amir Amirabadi, MohdNizam Ab Rahman, SoroushBaseriSaadi, AmirhosseinAghamohammadi, MersedehKooshkiForooshani, "Lung Infection Segmentation for COVID-19 Pneumonia Based on a Cascade Convolutional Network from CT Images", *BioMed Research International*, vol. 2021, ArticleID 5544742, 16 pages, 2021. <https://doi.org/10.1155/2021/5544742>
- [7] Khan, M.A.; Alhaisoni, M.; Tariq, U.; Hussain, N.; Majid, A.; Damaševičius, R.; Maskeliunas, R. - COVID-19 Case Recognition from Chest CT Images by Deep Learning, Entropy-Controlled Firefly Optimization, and Parallel Feature Fusion. *Sensors* 2021, 21, 7286. <https://doi.org/10.3390/s21217286>
- [8] IlkerOzsahin, BoranSekeroglu, Musa Sani Musa, Mubarak Taiwo Mustapha, DilberUzunOzsahin, "Review on Diagnosis of COVID-19 from Chest CT Images Using Artificial Intelligence", *Computational and Mathematical Methods in Medicine*, vol. 2020, Article ID 9756518, 10 pages, 2020. <https://doi.org/10.1155/2020/9756518>
- [9] AbdElaziz M, A. A. Al-qaness M, Abo Zaid EO, Lu S, Ali Ibrahim R, A. Ewees A (2021) Automatic clustering method to segment COVID-19 CT images. *PLoS ONE* 16(1): e0244416. <https://doi.org/10.1371/journal.pone.0244416>
- [10] Singh, Asu& Kumar, Anupam& Mahmud, Mufti & Kaiser, M. Shamim& Kishore, Akshat. (2021). COVID-19 Infection Detection from Chest X-Ray Images Using Hybrid Social Group Optimization and Support Vector Classifier. *Cognitive Computation*. (2021).1-13. 10.1007/s12559-021-09848- 3.

- [11]Deng-Ping Fan, Tao Zhou, Ge-Peng Ji, Yi Zhou, Geng Chen, Huazhu Fu, Jianbing Shen, Ling Shao"Inf-Net: Automatic COVID-19 Lung Infection Segmentation from CT Images"medRxiv 2020.04.22.20074948; doi: <https://doi.org/10.1101/2020.04.22.20074948>
- [12]Müller, Dominik & Soto-Rey, Iñaki& Kramer, Frank. (2021). Robust chest CT image segmentation of COVID-19 lung infection based on limited data. Informatics in Medicine Unlocked. 25. 100681. 10.1016/j.imu.2021.100681.
- [13]Elharrouss, O., Subramanian, N. & Al-Maadeed, S. An Encoder–Decoder- Based Method for Segmentation of COVID-19 Lung Infection in CT Images. SN COMPUT. SCI. 3, 13 (2022). <https://doi.org/10.1007/s42979-021-00874-4>
- [14]K. Gaurav, U. Ghanekar, Image steganography based on canny edge detection, dilation operator and hybrid coding, J. Inf. Secur. Appl. 41 (2018) 41–51.
- [15]R. Van Den Boomgaard, R. Van Balen, Methods for fast morphological image transforms using bitmapped binary images, CVGIP 54 (3) (1992) 252– 258.
- [16]B. Weng, M. Blanco-Velasco, K.E. Barner, Ecgdenoising based on the empirical mode decomposition. 2006 International Conference of the IEEE Engineering in Medicine and Biology Society, IEEE, 2006, pp. 1–4, <https://doi.org/10.1109/iembs.2006.259340>.
- [17]N.E. Huang, An Adaptive Data Analysis Method for Nonlinear and Nonstationary Time Series: The Empirical Mode Decomposition and Hilbert Spectral Analysis. Wavelet Analysis and Applications, Springer, 2006, pp. 363–376, https://doi.org/10.1007/978-3-7643-7778-6_25.
- [18]S. Naeem, A. Ali, S. Qadri, W. K. Mashwani, N. Tairan et al., “Machine- learning based hybrid-feature analysis for liver cancer classification using fused (MR and CT) images,” Applied Sciences, vol. 10, no. 9, pp. 3134–3160,2020.
- [19]A. Ali, S. Qadri, W. K. Mashwani, W. Kumam, P. Kumam et al., “Machine learning based automated segmentation and hybrid feature analysis for diabetic retinopathy classification using fundus image,” Entropy, vol. 22, no. 5, pp. 567–592, 2020.
- [20]Jan-Mark Geusebroek, R. van den Boomgaard, A.W.M. Smeulders, A. Dev, Color and scale: the spatial structure of color images, in: Proceeding of the 6th European Conference on Computer Vision, vol. 1, 2000, pp. 331–341.
- [21]Elharrouss O, Moujahid D, Tairi H. Motion detection based on the combining of the background subtraction and the structure–texture decomposition. Optik-Int J Light Electron Opt.2015;126(24):5992–7.
- [22]Elharrouss O, Moujahid D, Elkah S, Tairi H. Moving object detection using a background modeling based on entropy theory and quad-tree decomposition. Journal of Electronic Imaging. 2016;25(6): 061615.
- [23]Ronneberger O, Fischer P, Brox T. U-Net: convolutional networks for biomedical image segmentation. In: Lecture Notes in Computer Science. Springer, Berlin; 2015. p. 234–41.
- [24]Badrinarayanan V, Kendall A, Cipolla R. SegNet: a deep convolutional encoder-decoder architecture for image segmentation. IEEE Trans Pattern